CONCEPTUAL MODEL FOR CLOGGING IN UNSATURATED SOILS

P.J. Van Geel, Civil and Environmental Engineering, Carleton University, Ottawa
P. Kennedy, Civil and Environmental Engineering, Carleton University, Ottawa
M. Mostafa, Civil and Environmental Engineering, Carleton University, Ottawa

ABSTRACT
Bioclogging of unsaturated soils is an important concern in the design of biofilters to treat wastewater streams. Several conceptual models have been developed to simulate clogging in saturated soils, however, similar models have not been developed for unsaturated soils. This paper presents the results of a column study conducted to evaluate clogging in a peat biofilter. The results clearly illustrate the impacts of clogging with time on the vertical saturation profile within the filter. To simulate the clogging process, four conceptual models were proposed that link the microbial growth within the porous medium to the unsaturated relative permeability term. The models were incorporated into a one-dimensional unsaturated flow and transport code in which the biodegradation and microbial growth were simulated using Monod Kinetics. Initial model results illustrate the impacts of the microbial growth on the relative permeability term and the simulated saturation profile over time. Further research is needed to further develop and validate the proposed models.

RÉSUMÉ
L'obstruction biologique des sols insaturés est un aspect important dans la conception des biofiltres pour le traitement de l'écoulement des eaux usées. Plusieurs modèles conceptuels ont été développés pour simuler l'obstruction des sols saturés, toutefois il n'existe pas de modèles équivalents pour des sols insaturés. Cette publication présente les résultats d'une étude utilisant des colonnes pour évaluer l'obstruction des biofiltres à base de tourbe. Les résultats illustrent clairement l'impact de la progression de l'obstruction sur un profil vertical de saturation du filtre. Pour simuler le phénomène d'obstruction, quatre modèles conceptuels ont été proposés. Ces modèles font le lien entre l'activité microbienne en milieu poreux et le terme de perméabilité relative dans des conditions d'insaturation. Les modèles ont été incorporés dans un code de transport et de débit unidimensionel dans des conditions d'insaturation dans lequel la dégradation biologique et l'activité microbienne sont simulées en utilisant Monod Kinetics. Les résultats préliminaires du modèle illustrent les impacts de l'activité microbienne sur le terme de permeabilité relative et sur la progression du profile simulé de saturation. Des recherches plus approfondies sont nécéssaires pour développer et valider les modèles proposés.

1. INTRODUCTION

The processes impacting clogging of unsaturated soils have a significant impact on the performance of biofilters and septic systems. Several researchers have developed conceptual models for biological clogging in saturated flow systems. However, limited research has been completed to understand and develop similar conceptual models for biological clogging in unsaturated soils (Rockhold et al., 2002). The objectives of this ongoing research are to improve our understanding of the clogging process in unsaturated soils and to develop a conceptual model of this process for incorporation into an unsaturated flow and transport code.

This paper presents the results of a column study to evaluate the clogging of a peat biofilter. The influent was strictly a dissolved organic source and the resulting water content profiles and outflow rates over time indicate how the column clogged over time. The results form a data set against which numerical models can be validated.

The second part of this paper proposes several conceptual models of the clogging process. These conceptual models were incorporated into a one-dimensional unsaturated flow code to illustrate how each conceptual model simulates the clogging process.

2. PEAT COLUMN STUDY

The soil medium studied in this research was a peat used in a commercial peat biofilter to treat septic tank effluent from residential and small commercial sites. Six 0.5m-length and 0.162m-diameter peat columns of varying density were pulsed twice daily at a high organic loading rate. The dry density within the six columns varied between 110 and 180 kg/m^3. The hydraulic loading for each pulse was 0.097m and the water was added to the top of the column and then allowed to infiltrate under gravity drainage. The pressure head at the base of the peat columns was maintained at 0.09m of water suction. Glucose was used as the organic source and the influent concentration was 4395 mg/L. This resulted in an organic loading of 8.8 g/pulse or 17.6 g/day. The columns were pulsed each morning and afternoon, five days a week (Monday- Friday).

The water content profile was measured using TDR probes and the calibration curve developed for the same peat material. Over time, the apparent water content increased. This increase, which is discussed in greater

detail in the results section, is due to a fraction of the pore space being occupied by microbial growth. The microbial mass is approximately 80 per cent water by volume (Van Veen and Paul, 1979) and hence it was assumed that the TDR readings reflected the total water content, which is the actual water content and the water content of the microbial growth. Further study is warranted to investigate the impacts of microbial growth on the TDR readings.

A scale connected to a computer via an RS232 port, recorded the outflow with time from the column in response to a pulse.

Over a nine month period commencing on April 12, 2002, the columns were pulsed at the prescribed loading, the water content profiles within the columns were measured, and outflow rates in response to a pulse were recorded. The water content profiles were recorded just prior to the afternoon pulse. This allowed for consistent comparison of the water content profiles over time. The water content profile prior to the morning pulse would be slightly different and the profile on Monday morning would be different given that the columns were not pulsed on Saturday and Sunday.

3. COLUMN STUDY RESULTS

Over time the water content increased in the columns as clogging occurred. The outflow rate in response to a pulse also changed with time as the peat columns clogged. Columns A through F correspond to dry densities of 110 kg/m^3 to 180 kg/m^3, respectively. Figures 1, 2, and 3 present the water content profiles over time for three of the columns. The results of the remaining three columns are similar but are not provided due to space constraints. The impact of density on the water content profile can be seen when comparing the initial profiles measured on April 23, 2002. As expected, the water content profile is greater for the more dense columns as the greater density results in a smaller pore size distribution and a higher water content for a given capillary pressure or water suction. It is clear from these figures that as time progressed the water content increased as the microbial mass increased. The increase in microbial mass caused some of the water-filled pores to clog. As a result, the relative permeability decreased and the water content increased to compensate and allow the column to conduct the applied flow. Note that the water content profile does not reflect static conditions as the columns were pulsed 6 to 8 hours prior to the time when the TDR readings were taken.

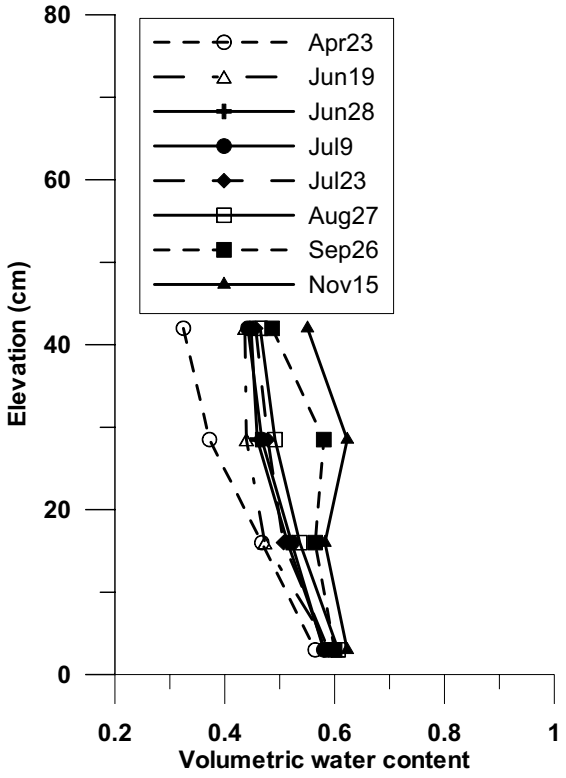

Figure 1. Water content profiles with time for Column A with density 110 kg/m^3.

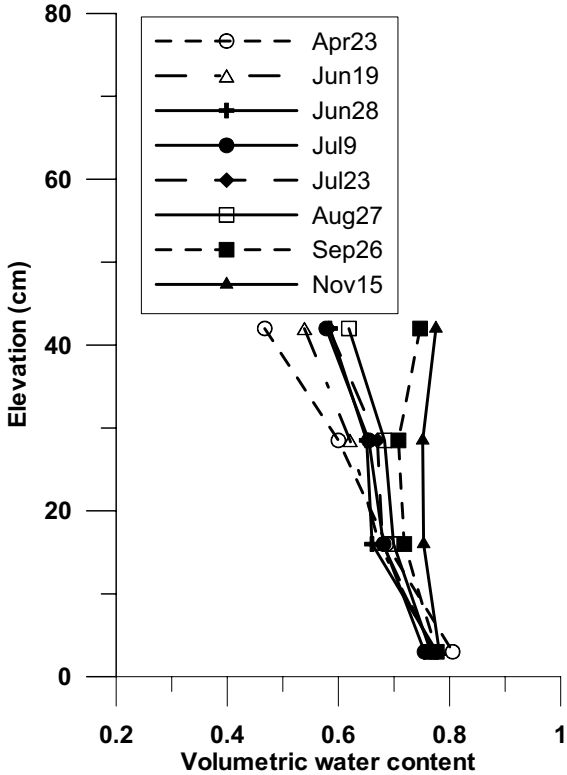

Figure 2. Water content profiles with time for Column C with density 140 kg/m^3.

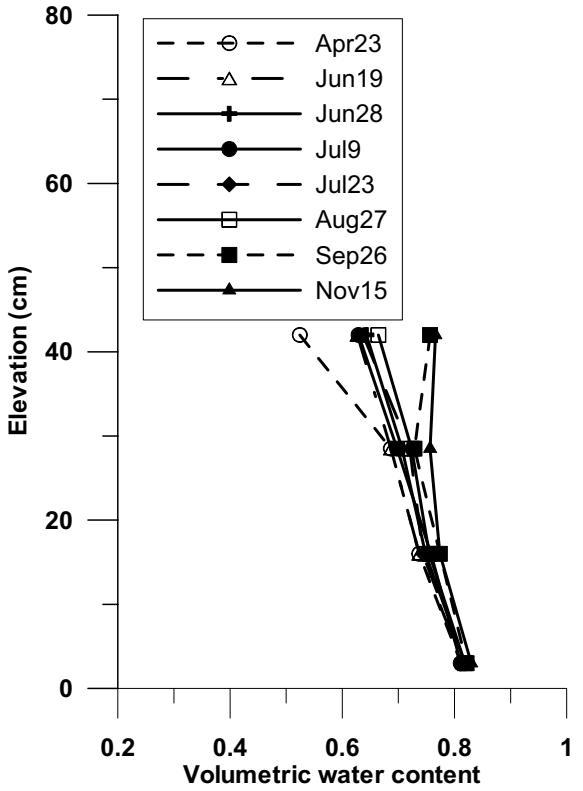

Figure 3. Water content profiles with time for Column F with density 180 kg/m^3.

The impact of the clogging on the outflow rates can be seen when comparing the outflow rates with time on June 11, 2002 (Figure 4) with the outflow rates with time on November 18, 2002 (Figure 5). As expected the outflow rates are impacted by dry density. For the least dense column, the hydraulic conductivity is greater and the influent pulse moves through the column faster. The differences between the outflow rates of columns A, B, and C are minimal on June 11, 2002 (Figure 4) and are substantial on November 18, 2002 (Figure 5). The outflow rates for columns D, E, and F are very low since these columns are nearly completely clogged and it takes 40, 1440 and 120 minutes for a pulse to infiltrate. For example, for Column F, the 0.097m pulse took 14 minutes to infiltrate in June and 120 minutes to infiltrate in November. A more extreme case was observed for Column E, which in June took 6 minutes for the 0.097m pulse to infiltrate, and 1440 minutes in November.

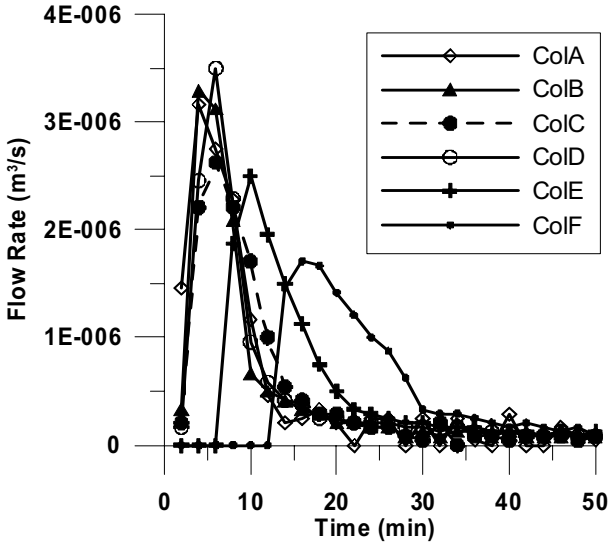

Figure 4. Outflow rate for columns A through F on June 11, 2002.

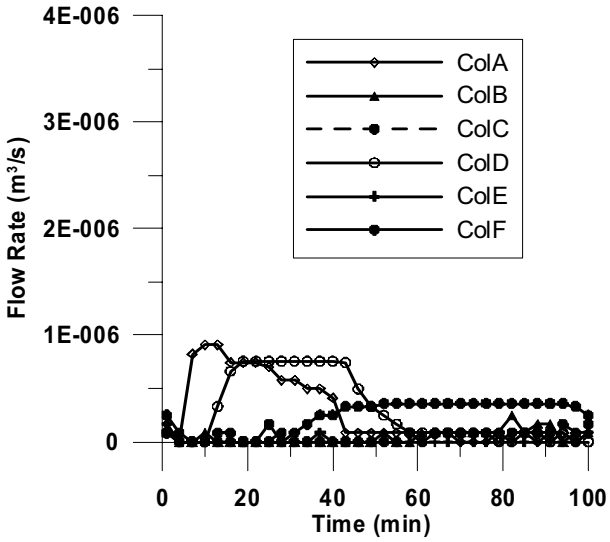

Figure 5. Outflow rate for columns A through F on November 18, 2002.

4. CONCEPTUAL MODEL FOR CLOGGING

Four conceptual models are proposed to relate the microbial growth to the relative permeability term in the unsaturated flow equation. The clogging process for saturated soils is different from that in unsaturated soils. In saturated soils, all the pores contribute to flow and various assumptions can be made with respect to the distribution of the microbial mass. Three conceptual approaches to modelling the clogging process in saturated soils have been identified: biofilm model, microcolony model and the strictly macroscopic model (Baveye et al., 1989) However, in unsaturated soils, not all the pores contribute to flow with the largest pores being the last to fill and contribute to

flow. Hence, a conceptual model needs to address this scenario. As the microbial mass increases, the water-filled pores clog and the relative permeability at that given saturation decreases. As a result, the water content increases to accommodate the flow. If the microbial mass continues to increase, the water content also continues to increase until saturated conditions are reached at which point ponding may occur to increase the hydraulic gradient since the permeability will only decrease. Hence, the proposed conceptual models have altered the relative permeability to account for the microbial mass.

Two common relationships are used to represent the relative permeability relationships in unsaturated soils. The relationship proposed by Burdine(1953)

$$k_r(S_{ew}) = S_{ew}^2 \left(1 - \left(1 - S_{ew}^{1/m}\right)^m\right) \quad [1]$$

and the relationship proposed by Mualem(1976)

$$k_r(S_{ew}) = S_{ew}^{1/2} \left(1 - \left(1 - S_{ew}^{1/m}\right)^m\right)^2 \quad [2]$$

Both relationships are based on the pressure-saturation relationship of van Genuchten (1980) where *m* is a fitting parameter (often *m=1-1/n: where n is a fitting parameter*) and S_{ew} is the effective water saturation. Similar equations can be generated for the Brooks and Corey (1964) relationship.

4.1 Model #1

The first and simplest conceptual model proposed involves reducing the relative permeability term by a factor of one minus the effective microbial saturation, S_{em}. An effective total saturation term, S_{et} , is also introduced to account for the volume of the pores occupied by the microbial mass. The new equations become:

$$k_r(S_{et}) = S_{et}^2 \left(1 - \left(1 - S_{et}^{1/m}\right)^m\right) . (1 - S_{em}) \quad [3]$$

and

$$k_r(S_{et}) = S_{et}^{1/2} \left(1 - \left(1 - S_{et}^{1/m}\right)^m\right)^2 . (1 - S_{em}) \quad [4]$$

4.2 Model #2

The second proposed model is based on the approach used by Lenhard and Parker (1987) in estimating the relative permeabilities of the water, air and immiscible fluid phases in a three phase flow system based on the assumed distribution of each phase in the pore space. In this approach, the integral relationships developed by Mualem and Burdine were modified to account for the presence of other phases including an entrapped phase. In the proposed formulation, the microbial mass is assumed to occupy a portion of the pore space as indicated in equation 5 based on Burdine and equation 6 based on Mualem.

$$k_r(S_{ew}) = S_{et}^2 \frac{\int_0^{S_{et}} \frac{dS_e}{\psi^2} - \int_0^{S_{em}} \frac{dS_e}{\psi^2}}{\int_{S_e=0}^{1} \frac{dS_e}{\psi^2}} \quad [5]$$

$$k_r(S_{ew}) = S_{et}^{1/2} \left(\frac{\int_0^{S_{et}} \frac{dS_e}{\psi} - \int_0^{S_{em}} \frac{dS_e}{\psi}}{\int_{S_e=0}^{1} \frac{dS_e}{\psi}} \right)^2 \quad [6]$$

The resulting relative permeability equations for Burdine and Mualem are

$$k_r(S_{ew}) = S_{et}^2 \left(\left(1 - S_{em}^{1/m}\right)^m - \left(1 - S_{et}^{1/m}\right)^m \right) \quad [7]$$

$$k_r(S_{ew}) = S_{et}^{1/2} \left(\left(1 - S_{em}^{1/m}\right)^m - \left(1 - S_{et}^{1/m}\right)^m \right)^2 \quad [8]$$

respectively. The approach can be seen graphically in Figure 6. One disadvantage of this approach is that based on equations 5 and 6, the microbial mass is assumed to fill the smallest pores (i.e. the pores between 0.0 and S_{em}) and these pores contribute the least to the relative permeability. This is discussed further in Section 4.5 Comparison of Proposed Models.

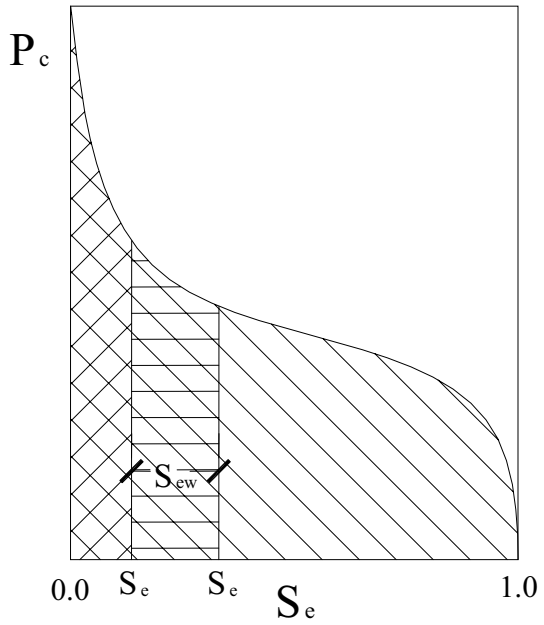

Figure 6. Saturation distribution assumed for relative permeability Model #2 where S_{ew} is the effective water saturation.

4.3 Model #3

The third and fourth approaches are based on a biofilm approach. The soil moisture curve is used to estimate the pore size distribution of the soil and the soil is assumed to reflect a bundle of capillary tubes. The saturation is divided into n equal incremental volumes. The average pore radius for each incremental volume is determined based on the average capillary pressure for that incremental volume. The number of capillary tubes and the total surface area associated with each incremental volume is then determined. The microbial mass is then assumed to distribute itself evenly over the surface area of the walls of the capillary tubes. For Model #3, the microbial mass is assumed to distribute itself evenly within all the pores or capillary tubes of the porous medium. The reduction in relative permeability is determined assuming laminar flow and the fact that the head losses are proportional to the square of the pore radii based on the Hagen-Poiseuille Equation. The resulting equation for Burdine follows:

$$k_r(S_{et}) = S_{et}^2 \left(1 - \left(1 - S_{et}^{1/m}\right)^m\right) \cdot \left(\frac{U_i\big|_0^{Porosity}}{U_o\big|_0^{Porosity}} \right) \qquad [9]$$

where the term on the right hand side is the ratio of the head losses with and without the biofilm based on equations 10 and 11.

$$U_o\big|_0^{Porosity} = \frac{\left(-\frac{\sum r^2}{8} \cdot \frac{\rho g}{\mu} \right)}{K_{sat}} \qquad [10]$$

$$U_i\big|_0^{Porosity} = \frac{\left(-\frac{\sum (r-t)^2}{8} \cdot \frac{\rho g}{\mu} \right)}{K_{sat}} \qquad [11]$$

where t is the estimated thickness of the biofilm if the microbial mass is distributed evenly within all the capillary tubes. The summation in equations 10 and 11 is the summation over all the pores between 0.0 and porosity (or S = 1.0). A similar equation can be generated for Mualem's relative permeability terms.

4.4 Model #4

The final model, Model #4, is similar to Model #3 with the exception that the biomass only distributes itself as biofilm in the water-filled pores. Hence, in equations 10 and 11, the summation for Model #4 is the summation over all the water-filled pores between 0.0 and S_{et}.

4.5 Comparison of Proposed Models

Table 1 illustrates the impact of a microbial mass on the relative permeability for each of the proposed models. For this example, the van Genuchten value for m was assumed to be 0.5, the effective microbial saturation was assumed to be 0.2, and the effective total saturation was assumed to be 0.8. The results are compared against the relative permeability for an effective water saturation of 0.8 without any biomass. As can be seen in Table 1, Models #1 and #4 had the largest impact on the relative permeability term. Model #2 predicted the least impact on the relative permeability term as it assumes that the smallest pores fill first and these contribute least to the permeability of the soil.

Table 1. Impact of microbial saturation on the estimated relative permeability for the four proposed models.

	k_r	k_r with S_{em} = 0.2 and S_{et} = 0.8			
	S_{em} = 0.0	M #1	M #2	M #3	M #4
Burdine	0.254	0.205	0.243	0.211	0.197
Mualem	0.143	0.114	0.129	0.118	0.110

Figures 7, 8 and 9 help illustrate the clogging process assumed for Models #2, #3, and #4.

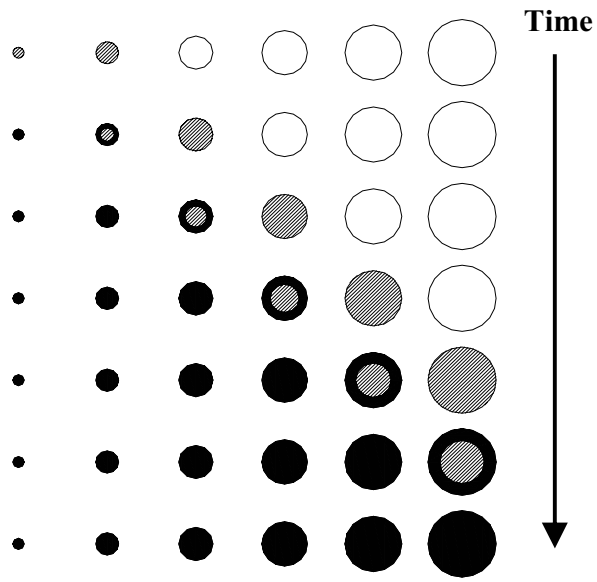

Figure 7. Conceptual view of the clogging process for Model #2

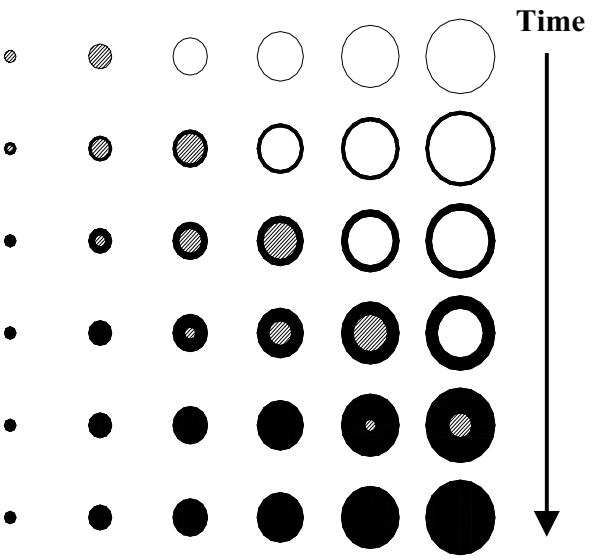

Figure 8. Conceptual view of the clogging process for Model #3

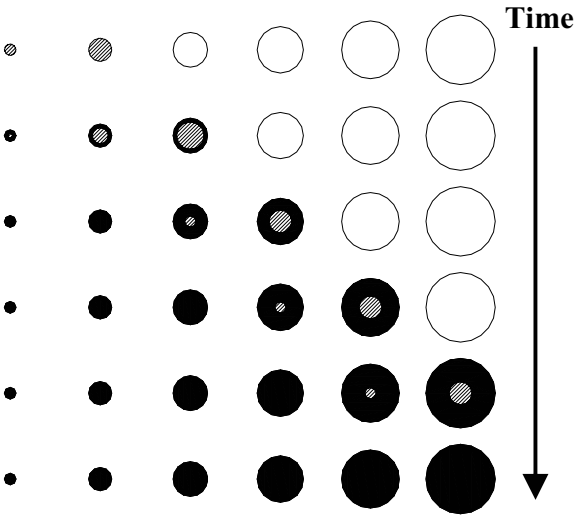

Figure 9. Conceptual view of the clogging process for Model #4

As illustrated in Figure 7, Model #2 allows the pores to clog sequentially starting with the smallest pore. This is reflected in the model formulation given in equations 5 and 6. Conceptually, this may not reflect the actual pore scale clogging process.

Figure 8 illustrates the clogging process assumed in Model #3. Once the microbial mass is known and a microbial volume determined, the microbial mass is distributed as a biofilm of uniform thickness t over the entire surface area of the pore space, which is represented as a set of capillary tubes. Hence, all the pore radii for the capillary tubes are reduced by the biofilm thickness. Since the head losses are proportional to the square of the radius, the relative permeability is reduced by the presence of the biofilm in all the capillary tubes.

A conceptual schematic of the clogging process for Model #4 is provided in Figure 9. As stated earlier, Model #4 is similar to Model #3 with the exception that the biomass is distributed as a biofilm over the water-filled pores and not the entire porosity. Hence, the result is a larger reduction in the pore radii contributing to flow and a larger reduction in the calculated relative permeability. This is evident in the values found in Table 1.

Further research and model validation is required to determine which model might best reflect the clogging process. However, to date, conceptual models that relate the microbial growth to the relative permeability term for clogging in unsaturated soils, have not been introduced in the literature.

5. 1D FLOW AND TRANSPORT MODEL

A one-dimensional unsaturated flow and transport code was developed. The unsaturated flow code is based on a non-hysteretic capillary pressure-saturation relationship. The contaminant transport code includes Monod kinetics to simulate the degradation of an organic substrate and the corresponding growth of the microbial mass. The equations used to simulate the transport and biodegradation follow:

$$\frac{\partial(\phi.S_w.C)}{\partial t}=\frac{\partial}{\partial z}\left(\phi.S_w.D_S.\frac{\partial C}{\partial z}\right)-\frac{\partial(q.C)}{\partial z}-\phi.S_w.R_s \qquad [12]$$

$$\frac{\partial C}{\partial t}=-R_s=-(M_T)(q_m)\left(\frac{C}{K_s+C}\right) \qquad [13]$$

where C is the organic substrate concentration, ϕ is porosity, S_w is the actual water saturation, D_S is the dispersion coefficient, q is the Darcy flux, M_T is the microbial concentration, q_m is the maximum rate of substrate utilization, and K_S is the half velocity constant.

The conservation of mass equation for the microbial growth is

$$\frac{\partial M_T}{\partial t}=(Y)(M_T)(q_m)\left(\frac{C}{K_s+C}\right)-(b)(M_T) \qquad [14]$$

where Y is the yield coefficient, and b is the microbial decay coefficient.

After determining the microbial mass, the volume occupied by this mass is calculated based on an assumed

density of 1.39 g/cm^3 (Robertson et al. 1998). The effective microbial saturation is then determined and relative permeability updated. The flow and transport equations are decoupled and the transport equation is solved explicitly with time.

The development of the code is ongoing and validation against the data presented herein was not complete at time of publication of this paper. However, a sample simulation is presented here to illustrate how the model works. For this simulation, a 1m peat column was discretized into 100 blocks of 1cm each. A continuous flux of 20cm/day was simulated at the top of the column and a constant pressure head of -9.9cm was used for the lower boundary condition. The saturated hydraulic conductivity and porosity are 0.079 cm/s and 0.8, respectively. The van Genuchten parameters for the irreducible water saturation, n and α are 0.08736, 1.3, and 0.18 cm^{-1}, respectively. The flow was initially simulated to establish steady state conditions. For the transport simulation, the concentration in the influent flux at the top of the column was 2000 mg/l. The dispersivity and molecular diffusion coefficients were 1cm and 0.00001 cm^2/s, respectively. The Monod parameters which include the maximum rate of substrate utilization (q_m), yield coefficient (Y), half-velocity constant (K_s), and the decay coefficient (b), were assumed to be 0.000005 mg BOD/mg cell-sec, 0.5 mg cells/mg BOD, 100 mg/l, and 0.000000578 sec^{-1} respectively. An initial microbial concentration of 1500 mg/l was assumed throughout the column.

The simulation results are presented in Figures 10 and 11. Figure 10 illustrates how the contaminant front advances with limited decay as the microbial mass increases with time. After 4 days (t3), the impact of the increased microbial mass at the top of the column (distance = 0 cm) can be seen. As time progresses, the microbial mass at the top of the column increases and the contaminant degradation rate increases. After 20 days, the contaminant concentration approaches zero at a depth of approximately 10 cm. However, the microbial growth is impacting the saturation profile as illustrated in Figure 11.

The initial saturation profile in the top 20 cm of the column is constant, approximately 0.75, due to gravity drainage and a vertical gradient of 1.0. As the microbial mass starts to develop, the total effective saturation remains close to the initial saturation. As discussed in section 4.2, an increase in the microbial saturation to 0.1 has little impact on the relative permeability term since the small pores below a saturation of 0.1 contribute very little to the total flow. For example, the relative permeability for an effective water saturation of 0.75 is 0.0049052 and the relative permeability based on equation 8 with an effective total saturation of 0.75 and an effective microbial saturation of 0.1 is 0.0049038. The difference is very small. Hence, the total effective saturation does not change to accommodate the flow of 20 cm/day and the effective water saturation decreases. At later times such as 42 days, the microbial saturation increases significantly and impacts the relative permeability term. As a result the total effective saturation increases to accommodate the flow. Eventually, the total effective saturation reaches 1.0 and the column becomes effectively clogged.

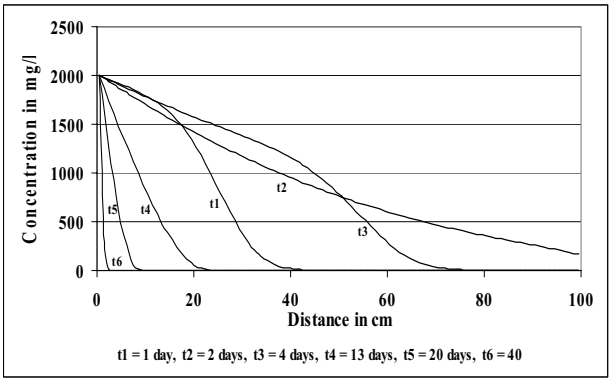

Figure 10. Concentration profiles within the column at 1, 2, 4, 13, 20 and 40 days.

For a continuous hydraulic loading of 20cm/day at 2000 mg/l, the simulation indicates that a biomass forms in the top 2-3 cm of the column. The model predictions based on Models #1, #3 and #4 predicted similar profiles. Model #1 predicted clogging to occur earlier since the effective microbial saturation has a larger impact on the relative permeability function. The predictions for Model #3 and #4 were similar to Model #2 since the impact on the relative permeability was similar. The trends follow those expected based on the impacts discussed in Table 1.

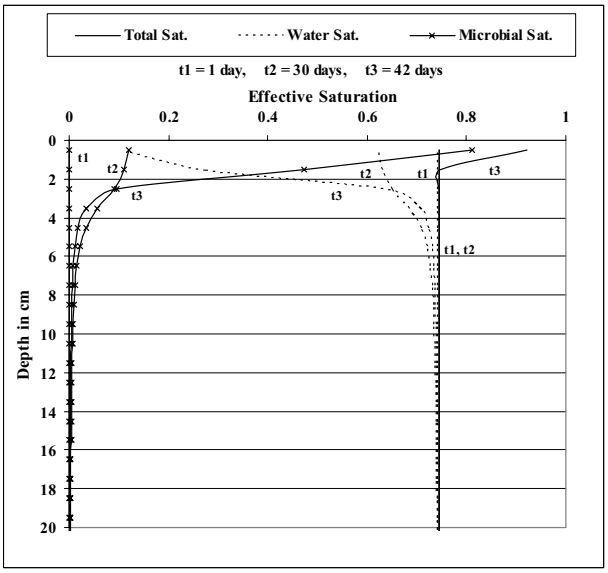

Figure 11. Effective Saturation profile with depth for the

6. CONCLUSIONS

Clogging in unsaturated soils is an important problem. Although there have been a number of conceptual models derived for saturated soils to help simulate the clogging process, very few have been proposed for unsaturated soils. Four conceptual models for clogging in unsaturated soils have been proposed in this research that link the microbial growth to the relative permeability term for unsaturated flow. The four models vary in complexity and approach. When incorporated into an unsaturated flow and transport code, the impacts of microbial growth on the water content profile can be simulated. Further experimental work and numerical modelling is needed to validate the proposed models.

The experimental data presented clearly illustrates the impact of microbial growth on the water content profiles over time as the soil clogs. The experiments provide a valuable validation data set for the proposed models. Efforts are ongoing to improve the existing model and to generate additional validation data.

7. REFERENCES

Baveye, P. and Valocchi, A. 1989. An evaluation of mathematical models of the transport of biologically reacting solutes in saturated soils and aquifers, Water Resources Research, Vol. 25, pp. 1413-1421.

Brooks, R.H. and Corey, A.T. 1964. Hydraulic Properties of Porous Media. Hydrological Papers, Vol. 3

Burdine, N.T. 1953. Relative Permeability Calculations from Pore Size Distribution Data. Transactions of the American Institute of Mining, Metal and Petroleum Engineering, Vol. 198, pp. 71-78.

Lenhard, R.J. and Parker, J.C. 1987. A Model for Hysteretic Constitutive Relations Governing Multiphase Flow 2. Permeability-Saturation Relations, Water Resources Research, Vol. 23, No. 21, pp.2197-2206.

Mualem, Y. 1976. A New Model for Predicting the Hydraulic Conductivity of Unsaturated Porous Media. Water Resources Research, Vol. 12, No. 3, pp. 513-522.

Robertson, B.R., Button, D.K. and Koch, A.L. 1998. Determination of the biomasses of Small Bacteria at Low Concentrations in a Mixture of Species with Forward Light Scatter Measurements by Flow Cytometry. Applied and Environmental Microbiology, vol. 64, No. 10, pp. 3900-3909.

Rockhold, M.L., Yarwood, R.R., Niemet, M.R., Bottomley, P.J. and Selker, J.S. 2002. Considerations for modelling bacterial-induced changes in hydraulic properties of variably saturated porous media. Advances in Water Resources, Vol. 25, pp. 477-495.

van Genuchten, M. Th. 1980. A Closed-form Equation for Predicting the Hydraulic Conductivity of Unsaturated Soils. Soil Science Society of America, Vol 44. pp. 892-898.

Van Veen, J.A. and Paul, E.A. 1979. Conversion of Biovolume Measurements of Soil Organisms, Grown Under Various Moisture Tensions, to Biomass and Their Nutrient Content. Applied and Environmental Microbiology, vol. 37, no. 4, pp. 686-692.